

# Heat Transfer and Friction Behaviour in a Channel with an Inclined Perforated Baffle

Ary Bachtiar Krishna Putra, Soo Whan Ahn\*<sup>†</sup>

Dept. of Mechanical System Engineering, Graduate School, Gyeongsang National University, Tongyong, 650-160, Korea (on leave from Sepuluh Nopember Institute of Technology, Indonesia).

\*School of Mechanical & Aerospace Engineering, Institute of Marine Industry, Gyeongsang National University, Tongyong, 650-160, Korea.

(Received January 17, 2008; Revision received May 30, 2008; Accepted June 17, 2008)

## Abstract

The effects of the inclined perforated baffles on the distributions of the local heat transfer coefficients and friction factors for air flows in a rectangular channel were determined for Reynolds numbers from 23,000 to 57,000. Four different types of the baffle are used. The inclined baffles have the width of 19.8 cm, the square diamond type hole having one side length of 2.55 cm, and the inclination angle of 5°, whereas the corresponding channel width-to-height ratio was 4.95. Results show that the heat transfer and friction factor depend significantly on the number of baffle holes and Reynolds number. The friction factor decreases with increasing Reynolds number and the number of holes on the baffle, and the heat transfer performance of baffle type II (3 hole baffle) has the best value.

*Key words:* Rectangular duct, Inclined baffle, Heat transfer, Friction factor, Square diamond type hole

## Nomenclature

$A$  : heat transfer area, m<sup>2</sup>  
 $c_p$  : specific heat of air, J/kg °C  
 $D_h$  : hydraulic diameter of the channel, m  
 $f$  : friction factor, see Eq.(1)  
 $h$  : heat transfer coefficient, W/m<sup>2</sup> °C  
 $H$  : test section height, m  
 $L$  : test section length, m  
 $\dot{m}$  : mass flow rate, kg/s  
 $Nu$  : Nusselt number,  $hD_h/k$   
 $Pr$  : Prandtl number  
 $\dot{Q}$  : Heat transfer rate, W  
 $Re$  : Reynolds number,  $u_b D_h/\nu$   
 $T$  : temperature, °C  
 $u$  : air velocity, m/s  
 $W$  : test section width, m  
 $x$  : distance from entrance of the heated test section, m

## Greek symbols

$\kappa$  : thermal conductivity of air, W/m °C  
 $\rho$  : air density, kg/m<sup>3</sup>

## Subscripts

$1$  : entrance  
 $2$  : exit  
 $b$  : Bulk, bottom  
 $ra$  : average value of channel  
 $s$  : side surface  
 $ss$  : empirical correlation for smooth channel  
 $t$  : top surface  
 $w$  : wall

## 1. Introduction

The baffle plate is usually attached to the heated surface to augment heat transfer by providing additional area for heat transfer and better mixing. This passive heat transfer enhancement strategy has been used for various types of industrial applications such as shell-and-tube type heat exchangers, electronic cooling devices, thermal regenerators, internal cool-

\*Corresponding author. Tel.: +82-55-640-3125, Fax.: +82-55-640-3128  
E-mail address: swahn@gaechuk.gunu.ac.kr

ing systems of gas turbine blades, and labyrinth seals for turbo-machines. This baffle can be used in solid or perforated manner.

Among important studies, Berner et al.<sup>1)</sup> obtained mean velocity and turbulence results in flow over baffles and Habib et al.<sup>2)</sup> investigated heat transfer and flow over the baffles having different heights. However, these works mainly emphasized on baffles perpendicular to the flow direction, therefore penalties (friction factor) were higher than the improvements on heat transfer.

Inserting inclined baffles in the flow path are well known technique to obtain enhancement on heat transfer with comparably less frictional head loss. Yilmaz<sup>3)</sup> experimentally investigated the heat transfer and associated frictional loss in the rectangular channel with inclined solid baffles for different inclination angle of 30, 45, and 60° to main flow direction. The results showed that the increase in the friction factor was much greater than that of the heat transfer. Recently, Dutta et al.<sup>4)</sup> reported heat transfer enhancement with an inclined perforated baffle. This paper showed better heat transfer augmentation with perforations compared to that with solid baffles, if the plate was attached to the heated surface and properly aligned in the direction of the flow. This baffle position was considered as a favorable orientation to enhance the local heat transfer coefficient up to five times of the results obtained in a smooth channel. For further study on perforated baffles Dutta et al.<sup>5)</sup> reported the analysis of heat transfer enhancement with the perforated baffles having inclination angles ranging from 3.8° to 9.6° to achieve optimum perforation densities and inclination condition. The results showed that the friction factor ratio decreases with a decrease in the angle of baffle and also with an increase in the perforation density. Moreover, friction factor ratio increases with an increase in the average Nusselt number ratio for a given configuration. Dutta et al.<sup>5)</sup> used simple circular holes as the baffle perforation types, in which the baffles have the width of 24.92 cm and the number of holes of up to 132, in addition, all the perforated baffles have comparatively small hole diameter of 1.07 cm. To the author knowledge, there are limited investigations dealing with the baffle hole diameter of over 1.5 cm and the hole geometry of diamond type.

Unlike previous publications, this paper dealt with experimental analysis of heat transfer enhancement and friction in the channel with different inclined

perforated baffles, having the baffle width of 19.8 cm and the square diamond type holes with one side large scale length of 2.55 cm. These baffles have the number of holes of up to 9 and the inclination angle of 5°.

## 2. Experimental facility

Fig. 1 shows a schematic diagram of the test apparatus. A suction-mode blower is used to draw air at room temperature through flow straighteners, passing through a long unheated straight rectangular channel with a cross-section of 19.8 cm[W] x 4 cm[H] and a length of 171.78 cm, finally through the heated test section of 71.2 cm. The channel has an aspect ratio[W/H] of 4.95, and hydraulic diameter of  $D_h = 6.66$  cm. The left, right and upper sides of the channel are made of 5-mm-thick transparent plexiglass plates, and the bottom side is made of 5-cm-thick wood plate. And the baffles are made of high temperature resistant acrylic plates. A total of twenty three so-flux stainless steel foil heaters of the same size of 198 mm x 30 mm x 0.1 mm(thickness) are mounted on the bottom surface of the test section. These foil heaters are aligned perpendicular to the flow direction and connected to a voltage controller to control the temperatures. Twenty three copper constantan thermocouples are laid along the heated test section centerline and glued at each strip of the foil heater using the thermal epoxy to measure the wall temperatures. Moreover, ten copper-constantan thermocouples are vertically distributed at the exit to measure the bulk temperature of air. The temperatures were monitored during heat-up period by data acquisition systems(Yokogawa DR230). After reaching thermal steady-state, all the temperature data were recorded on the storage device. Thermal energy lost is estimated from a separate heat-loss-experiment done on the test facility without air-flow. It is found that the maximum local heat flux loss,  $q''_{loss}$ , is less than 5% of the total local heat flux supplied,  $q''$ . All of the thermocouples used in the experiment are carefully calibrated to an accuracy of  $\pm 0.5^\circ\text{C}$ .

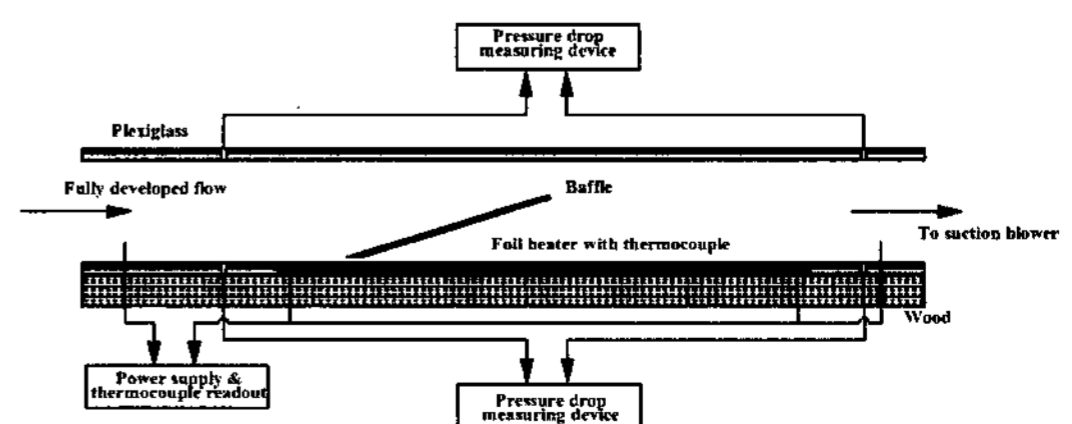


Fig. 1. Schematics of test apparatus.

Six pressure probes are used to measure pressure drops, and they are located at three positions of top, side, and bottom walls in 10 cm upstream of test section and three positions in 8 cm downstream test section. Since the pressure taps are located upstream and downstream of the actual test section, a correction on the pressure drop is performed based on the smooth channel analysis by the micro-manometer (FCO-12, Furness Control Ltd). A row of impingement holes is placed along the centerline of the perforated baffle to match the thermocouple locations. The air supply to the experimental apparatus was variable giving a range Reynolds number of 23,000 to 57,000 based on the hydraulic diameter  $D_h$  and flow bulk velocity  $u_b$ .

Details of the baffle position in the test section are shown in Fig. 2. All baffle types are mounted on the heated wall with a constant inclination angle of  $5^\circ$  and a gap ( $n$ ) of 4 mm between heated surface and the baffle is maintained to avoid flow stagnation and melting at the baffle plate contact. The baffle is placed at the position ( $m$ ) of 9.5 cm downstream from the start of the heated test section. Leading edge of the baffle is kept sharp to reduce possible flow disturbance by the protruding edge. All baffle types have the same overall size of length of 23.2 cm, width of 19.8 cm, and thickness of 5 mm. The schematic view of the baffle types used in this investigation is shown in Fig. 3. Four different types such as the solid baffle (baffle type I), the 3 hole baffle (baffle type II), the 6 hole baffle (baffle type III), and the 9 hole baffle (baffle type IV) were investigated, respectively. These square diamond holes having one side length,  $H_w = 2.55$  cm, transverse gap,  $S_w = 1.2$  cm, and longitudinal gap,  $S_l = 7.6$  cm were manufactured with laser

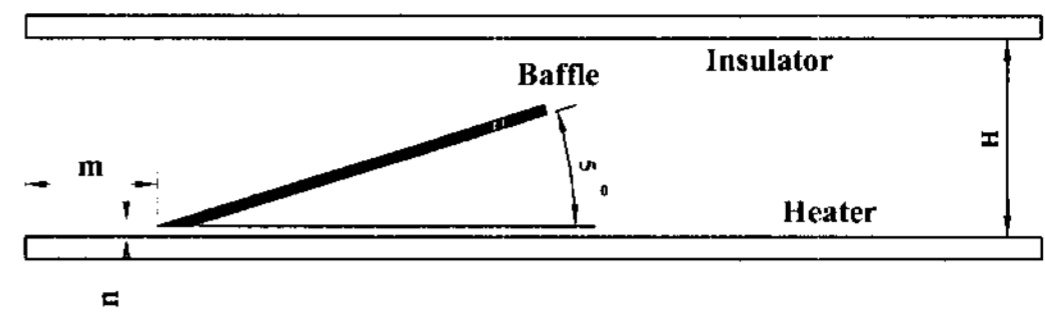


Fig. 2. Position of baffle in the test section.

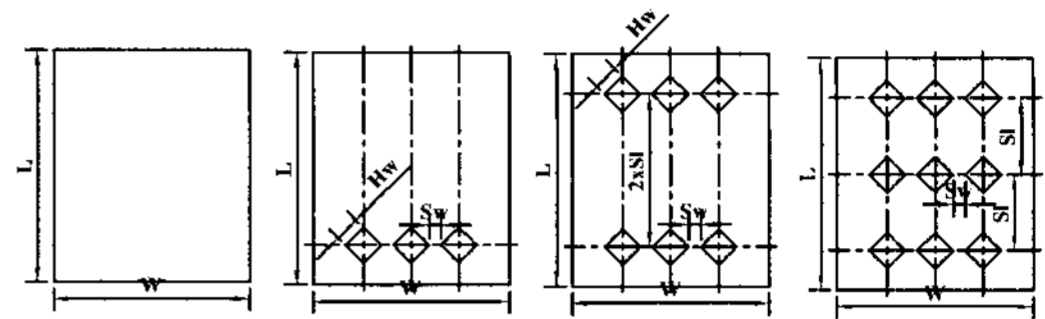


Fig. 3. Baffle plate configuration.

weld cutting. The experimental uncertainties are estimated using the procedure outlined by Kline and McClintock<sup>6</sup>. It is found in Table 1 that the uncertainties for Reynolds number, friction factor and Nusselt number are about  $\pm 2.5\%$ ,  $\pm 9.5\%$ , and  $\pm 7.8\%$ , respectively.

### 3. Data reduction

The friction factor in a rectangular channel can be defined by pressure drop  $\Delta p$ , and bulk mean air velocity  $u_b$  as follows:

$$f = \Delta p / [4(L/D_h)(\rho u_b^2 / 2)] \quad (1)$$

where the hydraulic diameter is  $D_h$ , and  $L$  is the length of the test section. The average channel friction factor  $f_{ra}$  is the average of the top wall friction factor  $f_t$ , the side wall friction factor  $f_s$  and the bottom wall friction factor  $f_b$ . The average friction factor for a rectangular channel can be expressed as:

$$f_{ra} = [W(f_t + f_b) + 2Hf_s] / (2W + 2H) \quad (2)$$

The average channel friction factor ( $f_{ra}$ ) is normalized using the friction factor for a fully developed turbulent flow in a smooth circular channel with the channel diameter replaced by the hydraulic diameter of the rectangular channel), as proposed by Blasius<sup>7</sup>:

$$f_{ra} / f_{ss} = f_{ra} / (0.079 Re^{-0.25}) \quad (3)$$

The local heat transfer coefficient is calculated from the net heat transfer rate per unit surface area exposed to the cooling air, the local wall temperature ( $T_w$ ), and

Table 1. Experimental uncertainties (Re=23,000).

Parameters	Uncertainties
Thermophysical property of air	$\pm 2.0\%$
Hydraulic diameter, $D_h$	$\pm 0.5\%$
Bulk velocity, $u_b$	$\pm 1.5\%$
Pressure difference, $\Delta P$	$\pm 9.2\%$
Reynolds number, $Re$	$\pm 2.5\%$
Friction factor, $f$	$\pm 9.5\%$
Temperature, $T$	$\pm 0.5^\circ\text{C}$
Heat transfer coefficient, $h$	$\pm 7.5\%$
Nusselt number, $Nu$	$\pm 7.8\%$

the local bulk mean air temperature ( $T_b$ ) as follows :

$$h = \dot{Q} / [A(T_w - T_b)] \quad (4)$$

where  $A$  is the total heat transfer area of the heated wall. The net heat transfer rate ( $\dot{Q}$ ) is defined as:

$$\dot{Q} = \dot{m}c_p(T_{b2} - T_{b1}) \quad (5)$$

where  $T_{b1}$  and  $T_{b2}$  represent the fluid bulk temperatures at the entrance and exit, respectively. The local Nusselt number is defined using the local heat transfer coefficient and the hydraulic diameter  $D_h$  for the rectangular channel:

$$Nu = hD_h / k \quad (6)$$

The aim of the work is to quantify the enhancement to the internal heat transfer coefficients in the channel in terms of inclined perforated baffles. All of the enhancement factors were obtained by normalizing the local heat transfer coefficients measured by that along the centerline of the passage in the absence of the baffles correlated by McAdams/Dittus-Boelter<sup>7)</sup> as:

$$Nu / Nu_{ss} = (hD_h / k) / (0.023Re^{0.8}Pr^{0.4}) \quad (7)$$

And the average Stanton number is given by:

$$St = Nu / (Re.Pr) \quad (8)$$

The Reynolds number was calculated on the basis of channel average velocity and channel hydraulic diameter. The channel average velocity was derived from flow rate of the circular tube at downstream of test section.

#### 4. Results and discussion

Fig. 4 shows the channel-averaged friction factors obtained from the experimental data for all baffle types at ten different Reynolds numbers ranging from 23,000 to 57,000. Before initiating experiments with inclined baffles, the friction factor was measured for smooth channel with no baffles as a reference.

The empirical equation by Blasius for a smooth circular tube<sup>7)</sup> is included for a comparison. Our results for a smooth channel with no baffle coincide well with the Blasius' correlation within 7% deviation.

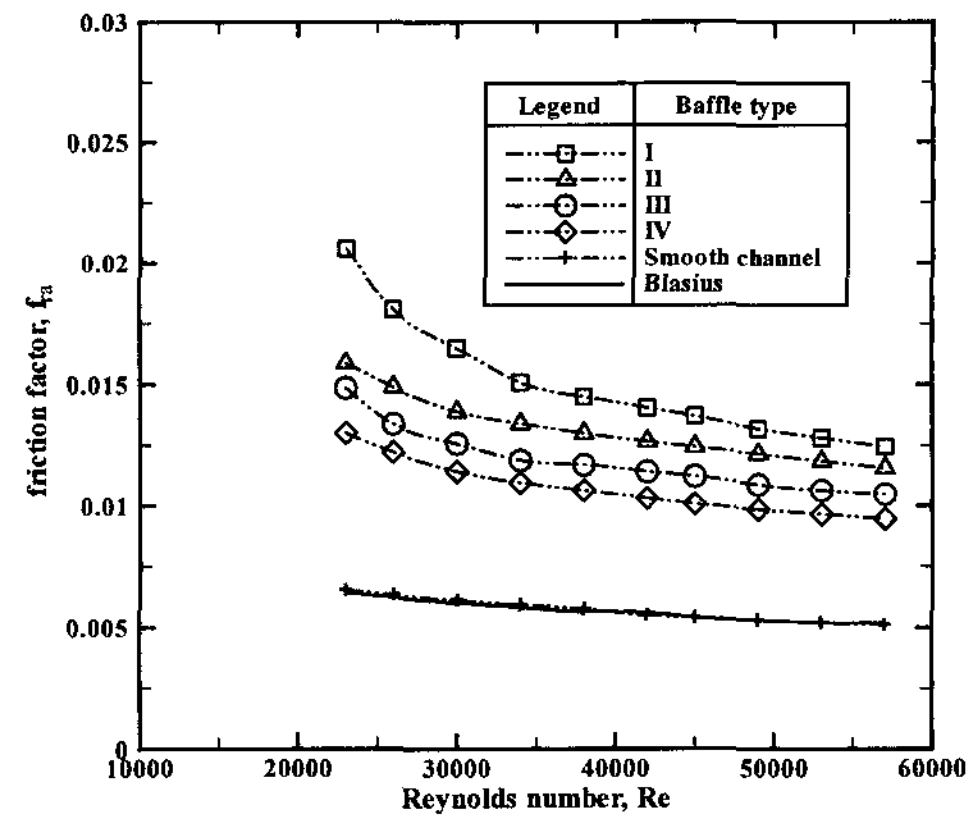


Fig. 4. Friction factor.

The friction factor decreases with increasing Reynolds number since a relative increase in the magnitude of kinetic energy is greater than an increase in wall shear stress. The friction factor of the solid baffle (baffle type I) is highest due to the worst blockage of bulk flow.

Figs. 5-8 show the Nusselt number ratio  $Nu/Nu_{ss}$  for different baffle plates (different perforation density) placed at the same location in the channel. These Nusselt number ratios indicate the amount in heat transfer coefficient obtained by these baffles over a fully developed smooth channel condition. In the present work, heat transfer coefficient for smooth duct was also determined to be within 9.5% deviation from literature values<sup>7)</sup>.

Fig. 5 shows the centerline local Nusselt number ratio ( $Nu/Nu_{ss}$ ) distributions with solid baffle (type I) obtained from equation (7). The local Nusselt number ratio is comparatively high at the start of heating test section. It is due to the starting of the thermal boundary layer development. Local  $Nu/Nu_{ss}$  peaks takes place at  $x/D_h=2.2$ . This occurs because the gap between the baffle leading edge and the heating wall (bottom wall) creates the sudden contraction effect. Near the trailing end of the baffle, the downward trend of Nusselt number ratio is due to a divergent orientation of the baffle decreasing the local air velocity. Sharply decreasing on the Nusselt number ratio immediately after the end of the baffle occurs due to recirculation effect, and then the ratio suddenly increases while flow reattachment occurs. Further downstream the heat transfer behavior approaches the channel condition with no baffle.

Fig. 6 represents the normalized Nusselt numbers

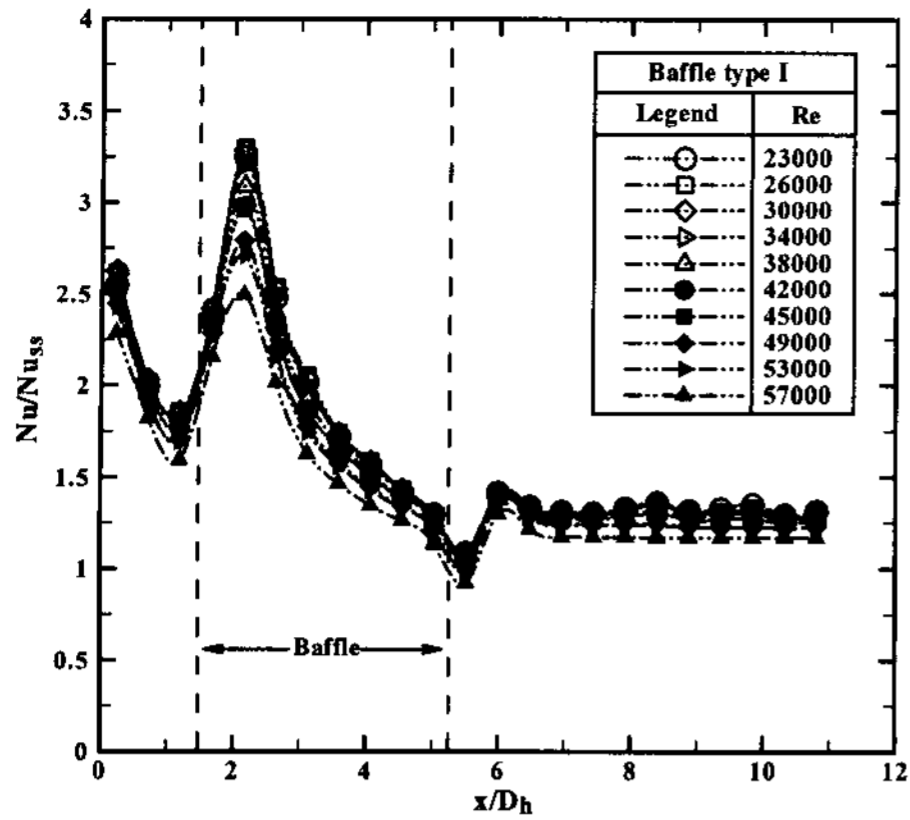


Fig. 5. Local Nusselt numbers for type I.

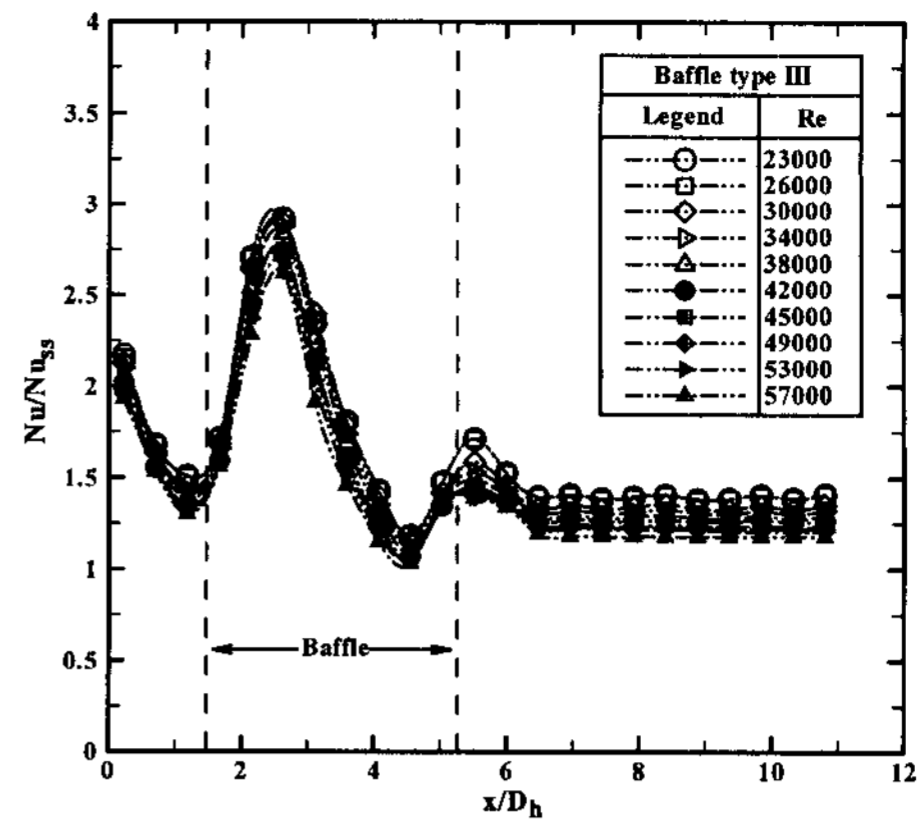


Fig. 7. Local Nusselt numbers for type III.

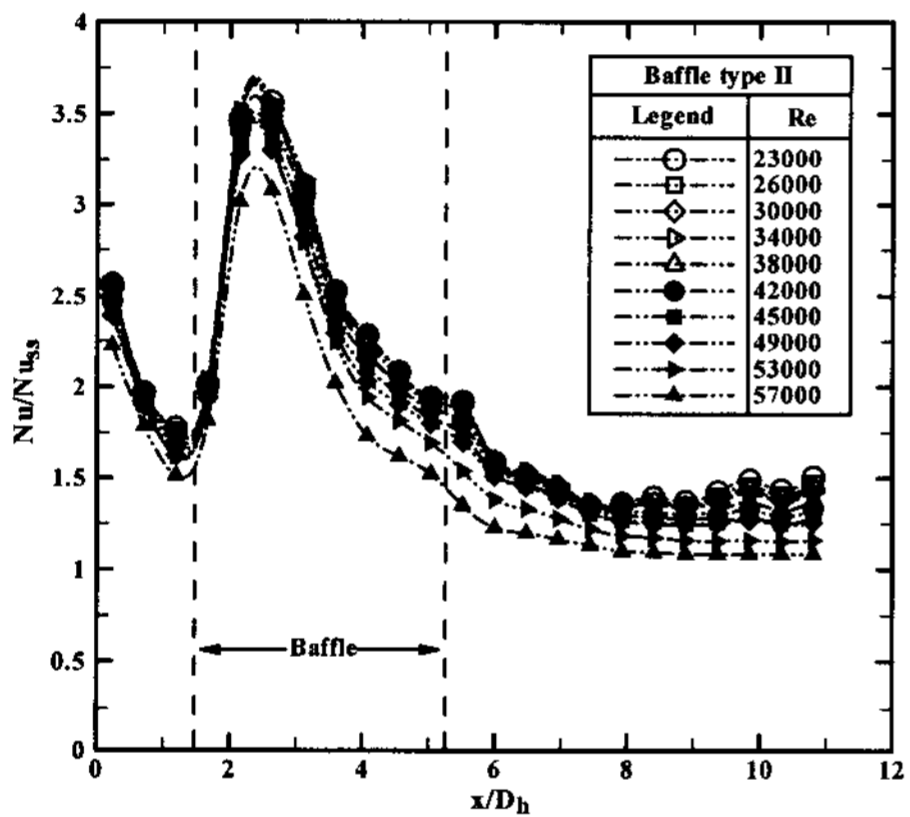


Fig. 6. Local Nusselt numbers for type II.

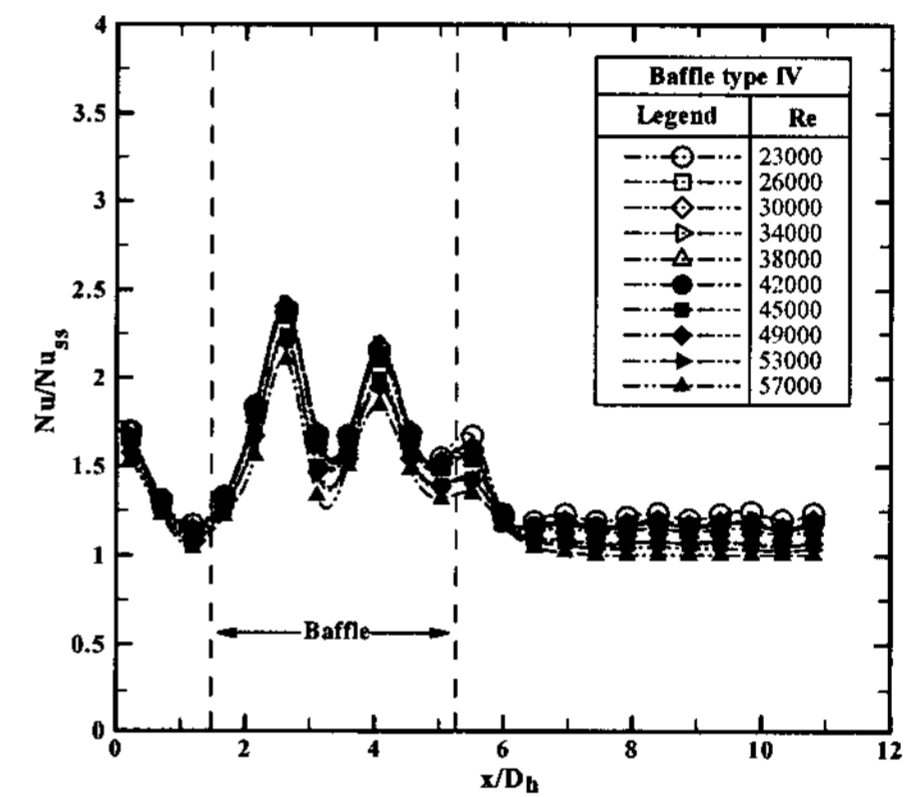


Fig. 8. Local Nusselt numbers for type IV.

for baffle type II having 3 holes. The local  $Nu/Nu_{ss}$  peaks of the channel for baffle type II are higher than those of the baffle type I (solid baffle). This is due to the jet impingement effect that can improve flow momentum. Another heat transfer behavior distinction between two baffle types is that downward trend of Nusselt number ratio of the baffle type II is more gentle than that of the baffle type I (solid baffle) because no flow recirculation occurs on the downstream of baffle type II.

Fig. 7 shows the centerline local Nusselt number ratio distributions of the channel for baffle type III as a function of the dimensionless axial location  $x/D_h$ . This figure shows that the Nusselt number ratio distributions of the channel for baffle type III at the start of the heated section are lower than baffle type I and II. It is because the boundary layer disturbance is weaker. The local  $Nu/Nu_{ss}$  peaks are due to the jet impingement effect. However, dissimilar with the baffle type II, the holes near trailing end of baffle III

create the secondary peaks of  $Nu/Nu_{ss}$  immediately after the end of the baffle. It is attributed to the fact that the divergent orientation of the baffle creates higher inclination of impinging jet flow in the impact zone at this location.

Fig. 8 presents the local Nusselt number ratio distribution at the centerline of the channel for baffle type IV. There are three peaks of the local  $Nu/Nu_{ss}$  in the channel due to the multiple impingement effect. These peaks have a relatively lower heat transfer enhancement compared with three other baffle types. It can be argued that the impingement effect is weaker in the baffle with more perforations.

Fig. 9 shows the average Nusselt number ratio ( $Nu_{avr}/Nu_{ss}$ ) for different baffle types at various Reynolds numbers. The subscript *avr* means the channel averaged values. The baffle type II has the highest average Nusselt number ratios. An interesting observation is that Nusselt numbers aren't highest at the most number of holes. It may be deserved that a

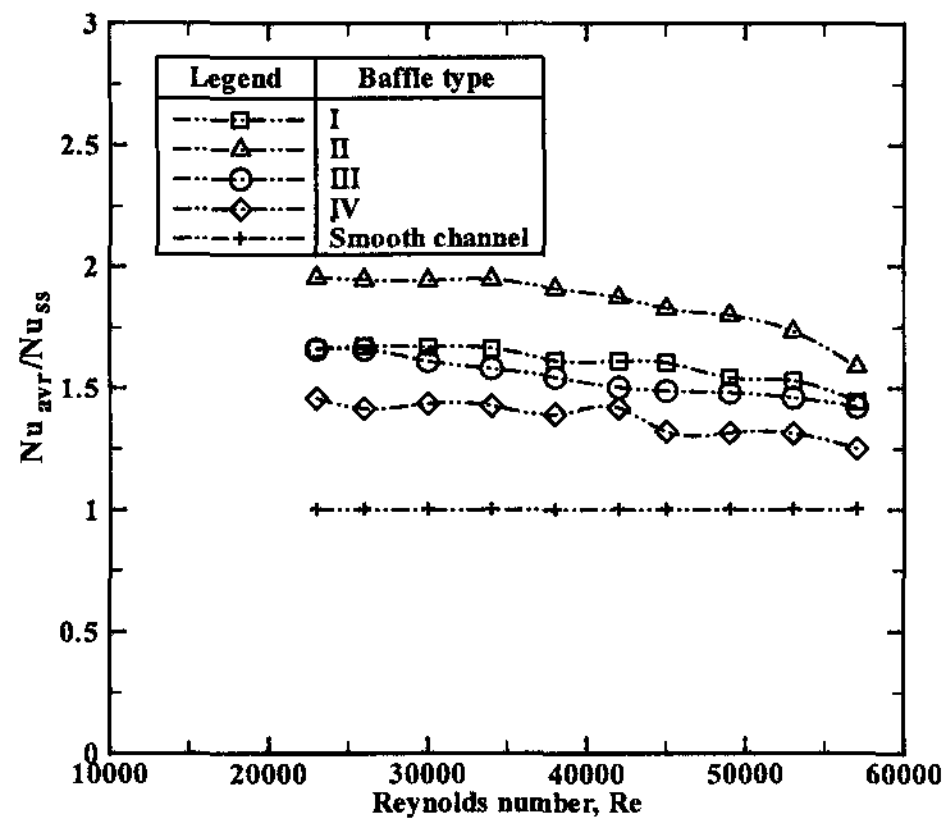


Fig. 9. Normalized Nusselt numbers.

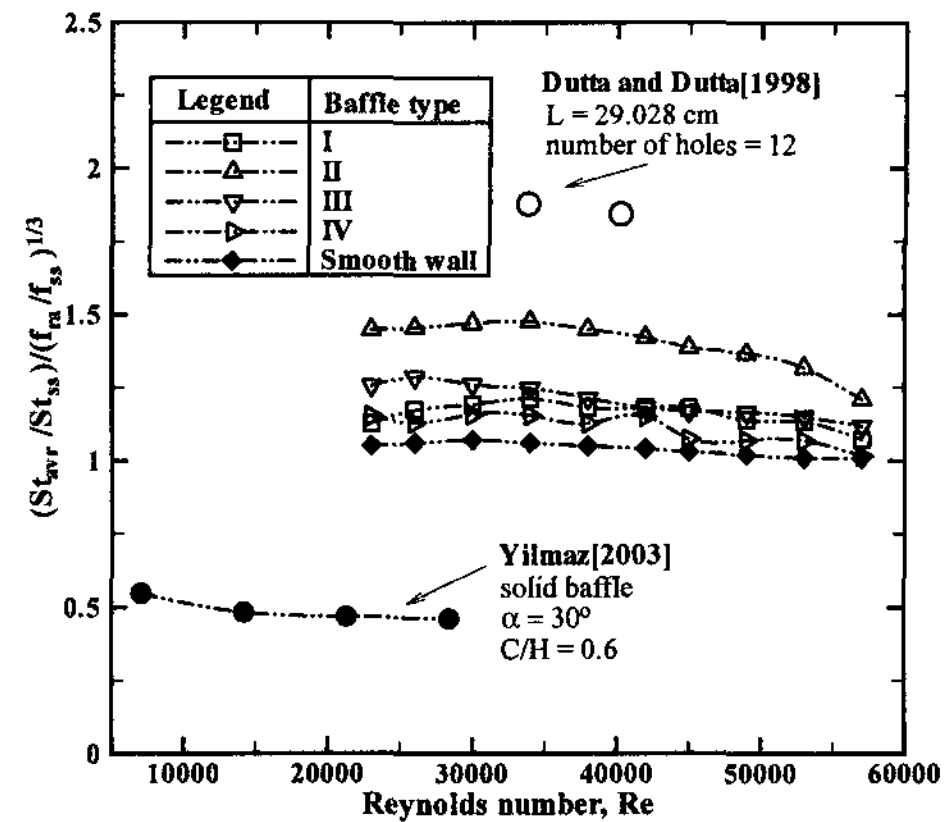


Fig. 11. Heat transfer performance.

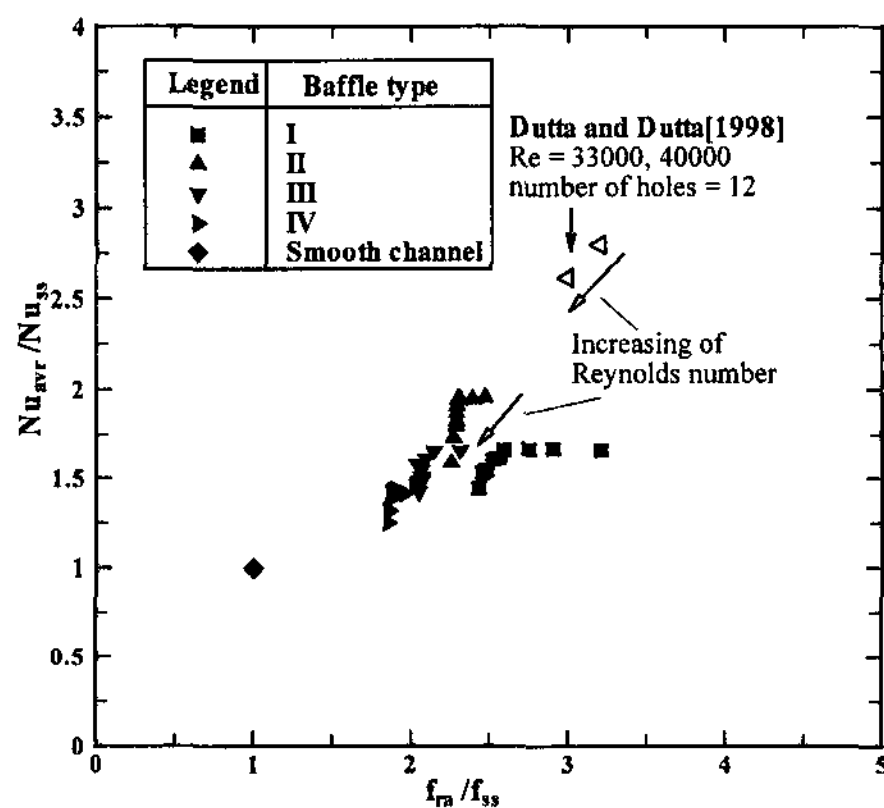


Fig. 10. Qualitative performance.

more number of holes increases the cross flow by spent jets and reduces impingement effect.

Fig. 10 represents the qualitative performance. The experimental results by Dutta et al.<sup>5)</sup> are included for a comparison. The values of present study are considerably lower than results of Dutta et al. It is attributed to the different geometric shape, i.e., Dutta et al. used the baffle with a smaller circular hole diameter of 1.07 cm and a more number of holes of 12. However, the present work used the baffle with square diamond type holes having one side length of 2.55 cm and the hole number of up to 9.

Fig. 11 shows the heat transfer performance under a constant pumping power. The variations in the values of heat transfer performance are 0.98-1.24, 1.17-1.49, 1.07-1.29, and 0.99-1.19 for baffle type I, II, III, and IV, respectively. This figure also includes the experimental results by Yilmaz<sup>3)</sup> and Dutta<sup>5)</sup> as comparison. Yilmaz<sup>3)</sup> conducted an experimental study for the 30°

inclined baffle in the rectangular channel. The results of Yilmaz are considerably lower than ours. It is supposed that the higher baffle inclination angle can create extremely higher friction factor. The values of Dutta et al. also show a higher heat transfer performance rather than the present study. It can be reasoned that the better impingement creates a significant enhancement of heat transfer against the pressure drop penalty.

## 5. Conclusions

This paper investigated heat transfer and friction characteristics in rectangular channel with a single inclined baffle and the flow Reynolds number was varied between 23,000 and 57,000. Four samples having different number of holes in the baffle were tested. Listed below are major findings:

- 1) The friction factor of the solid baffle (baffle type I) were highest due to the worst blockage of bulk flow.
- 2) The baffle type II had the highest average Nusselt number ratios. The additional holes in the perforated baffle reduce the jet impingement effect, hence reducing the heat transfer enhancement.
- 3) The best heat transfer performance occurred at the rectangular channel with baffle type II, which had a maximum of 1.49 times greater than that of the channel with no baffle at  $Re = 57,000$

## Acknowledgements

This work was supported by the New University for Regional Innovation Projects.

**References**

- [1] Berner, C., Durst, F., and McEligot, D. M., 1984, Flow around baffles, ASME J. Heat Transfer, Vol. 106, pp. 743 -749.
- [2] Habib, M. A., Mobarak, A. M., Sallak, M. A., Abdel Hadi, E. A., and Affify, R. I., 1994, Experimental investigation of heat transfer and flow over baffles of different heights, ASME J. Heat Transfer, Vol. 116, No. 2, pp. 363-368.
- [3] Yilmaz, M., 2003, The effect of inlet flow baffles on heat transfer, Int. Comm. Heat Mass Transfer, Vol. 30, No. 8, pp. 1169-1178.
- [4] Dutta, S., Dutta, P., Jones, R. E., and Khan, J. A., 1997, Experimental study of heat transfer coefficient enhancement with inclined solid and perforated baffles, Int. Mech. Engineering Congress and Exposition, ASME Paper No. 97-WA/HT-4, November 16-21, Dallas, Texas.
- [5] Dutta, P., and Dutta, S., 1998, Effect of baffle size, perforation and orientation on internal heat transfer enhancement, Int. J. Heat Mass Transfer, Vol. 41, No. 19, pp. 3005-3013.
- [6] Kline, S. J., and McClintock, F. A., 1953, Describing uncertainty in single sample experiments, Mechanical Engineering, Vol. 75, pp. 3-8.
- [7] Kays, W. M., and Crawford, M. E., 1990, Convective heat and mass transfer, 2nd ed., McGraw-Hill, New York.